

Contrast Enhancement by Multi-scale Adaptive Histogram Equalization

Yinpeng Jin^a, Laura Fayad^b and Andrew Laine^{*a}

^aDepartment of Biomedical Engineering, Columbia University, New York, NY

^bDepartment of Radiology, Columbia-Presbyterian Medical Center, New York, NY

ABSTRACT

An approach for contrast enhancement utilizing multi-scale analysis is introduced. Sub-band coefficients were modified by the method of adaptive histogram equalization. To achieve optimal contrast enhancement, the sizes of sub-regions were chosen with consideration to the support of the analysis filters. The enhanced images provided subtle details of tissues that are only visible with tedious contrast/brightness windowing methods currently used in clinical reading. We present results on chest CT data, which shows significant improvement over existing state-of-the-art methods: unsharp masking, adaptive histogram equalization (AHE), and the contrast limited adaptive histogram equalization (CLAHE). A systematic study on 109 clinical chest CT images by three radiologists suggests the promise of this method in terms of both interpretation time and diagnostic performance on different pathological cases. In addition, radiologists observed no noticeable artifacts or amplification of noise that usually appears in traditional adaptive histogram equalization and its variations.

Keywords: Contrast Enhancement, Adaptive Histogram Equalization, Over-complete Multi-scale Analysis, Spline Wavelets.

1. INTRODUCTION

1.1 Chest CT Diagnosis with Conventional Window-level Reading

Contemporary medical imaging modalities such as computed tomography (CT), magnetic resonance imaging (MRI), and digital radiography often contain 12 bits or more of significant contrast information. Anatomical tissues may occupy significantly different dynamic ranges on display due to difference of X-ray attenuation. By comparison, the human visual system can only perceive less than 100 different gray levels [1]. Thus, contrast enhancement is usually needed for clinical readings. Linear intensity windowing techniques are the simplest and most commonly used method [2].

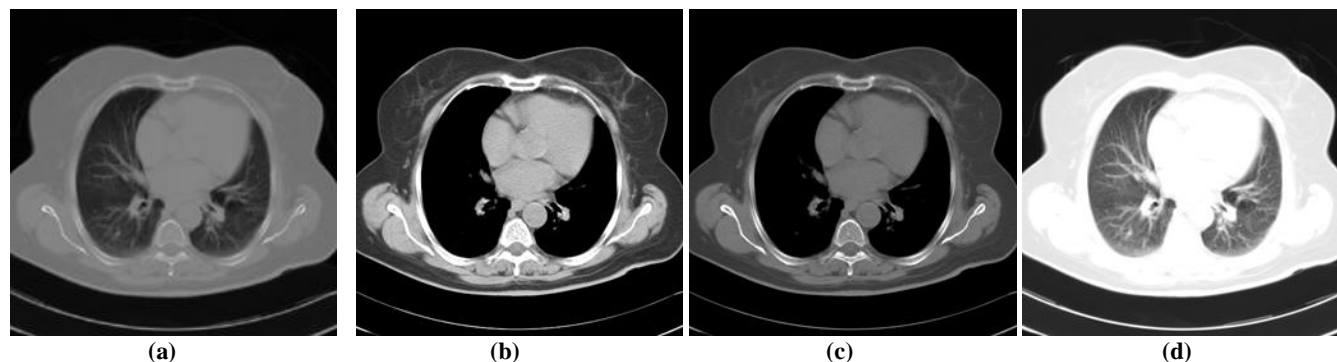


Figure 1: A chest CT image (a), and three brightness/contrast settings specific for (b) soft tissue, (c) bone and (d) lung.

For example, the chest CT usually contains three distinct tissues of clinical interest: Soft tissue, Lung and Bone. Conventionally, three settings of brightness/contrast for display are used (Figure 1) to generate three different views for reading (with settings specific for enhancing soft tissue, bone and lung details). This process of selecting parameter values and interpreting resultant windowed CT images is time consuming, even with the advent of digital imaging and displays that allows window settings to be varied rather quickly via an interactive console. Thus, the ability to visualize a CT image with these three dynamic contrast ranges simultaneously would result in an economical, efficient and automatic method of CT interpretation. The radiologists could therefore focus on all tissues in a single image without necessitating a change of window level and center parameters.

* Correspondence: laine@columbia.edu

1.2 Contrast Enhancement by Histogram Equalization and Its Variations

In some CT radiographs, the features of interest occupy only a relatively narrow range of the gray scale. Contrast enhancement is a method to expand the contrast of features of interest so that they occupy a larger portion of the displayed gray level range without distortion to other features and the overall image quality. The goal of contrast enhancement techniques is to determine an optimal transformation function relating original gray level and the displayed intensity such that contrast between adjacent structures in an image is maximally portrayed [3]. A review of traditional contrast enhancement methods for digital radiography can be found in [4].

The histogram of an image represents the relative frequency of occurrence of gray levels within an image. Histogram-modeling techniques modify an image so that its histogram has a desired shape. This is useful in stretching the low-contrast levels of an image with a narrow histogram, thereby achieving contrast enhancement. In histogram equalization (HE), the goal is to obtain a uniform histogram for the output image, so that an “optimal” overall contrast is perceived. However, the feature of interest in an image might need enhancement locally. And although there was no decrease in detectability of simulated low contrast live metastases for an experienced reader [5], radiologists always find the appearance of the HE-enhanced images to be objectionable in that they often introduce undesirable artifacts and noise [6].

Adaptive Histogram Equalization (AHE) computes the histogram of a local window centered at a given pixel to determine the mapping for that pixel, which provides a local contrast enhancement [7]. However, the enhancement is so strong that two major problems can arise: noise amplification in “flat” regions of the image and “ring” artifacts at strong edges [1].

A generalization of AHE, contrast limiting AHE (CLAHE) has more flexibility in choosing the local histogram mapping function. By selecting the clipping level of the histogram, undesired noise amplification can be reduced [8]. In addition, by method of background subtraction, the boundary artifacts can also be reduced [9].

1.3 Contrast Enhancement using Over-complete Dyadic Spline Wavelets

Unlike traditional single scale techniques, wavelet-based algorithms offer the capability of modifying/enhancing image components adaptively based on their spatial-frequency properties. Non-redundant multi-scale representations lack translation invariance and present aliasing after the decomposition stage due to down-sampling [10], and motivate our usage of an over-completed wavelet representation [11, 12].

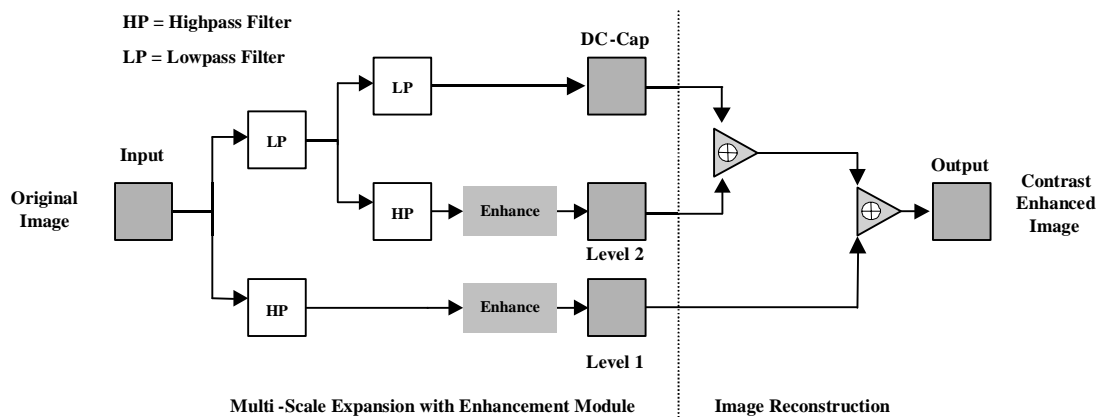


Figure 2: Multi-scale analysis with non-linear contrast enhancement: Schematic of a filter bank implementation. Left: multi-scale expansion with enhancement for 2 levels of analysis is shown, Right: reconstruction presented in a simplified manner.

The general framework of a filter bank implementation of an over-complete multi-scale enhancement is schematically illustrated in Figure 2, for a two level decomposition. Redundancy was exploited for image enhancement by first modifying transform coefficients in the transform domain and then reconstructing. Notice that since the DC-Cap contains much of the energy distribution, and is usually not modified during the enhancement procedure [12]. As shown above, the enhancement function can be implemented independently of a particular set of filters and easily incorporated into a filter bank to provide the benefits of multi-scale enhancement [13, 14].

The discrete dyadic wavelet transform is one example of a redundant representation, in which case the scale parameter is discretized to the dyadic sequence $\{2^j\}$ with $j \in \mathbb{Z}$, and the translation parameter is sampled with the same sampling period as the input image, over all scales [15]. The 2-D dyadic wavelet transform partitions orientations into two sub-bands

corresponding to the horizontal and vertical components respectively. The wavelet transform of a 2D signal $f(x, y)$ at scale $\{2^j\}$ has two component defined by:

$$W_{2^j}^1 f(x, y) = f * \psi_{2^j}^1(x, y) \text{ and } W_{2^j}^2 f(x, y) = f * \psi_{2^j}^2(x, y), \text{ with } \psi_{2^j}^d(x, y) = \frac{1}{\sqrt{2^j}} \psi^d\left(\frac{x}{2^j}, \frac{y}{2^j}\right), d = 1, 2.$$

The enhanced sub-band images \hat{y}_j^i may be given by:

$$\hat{y}_j^i = f_i(y_j^i) \tag{1}$$

where f_i is a set of user-defined monotonically increasing positive functions designed to emphasize features of importance within some level i . The enhanced sub-band coefficients \hat{y}_j^i are then used to reconstruct the output images. In general, by defining a function f_i , we can denote specific enhancement schemes for modifying sub-band image coefficients within distinct levels of a scale space.

2. METHOD

2.1 Multi-scale Adaptive Histogram Equalization (MAHE)

Adaptive histogram equalization (AHE) uses the HE mapping function supported over a certain size of a local window to determine each enhanced density value. It acts as a local operation. Therefore regions occupying different gray scale ranges can be enhanced simultaneously. As we mentioned in the first section, it performs so aggressive that in relatively homogeneous areas the noise becomes very prominent. As the only parameter, the size of the local window controls the trade-off between local enhancement and noise amplification. The AHE algorithm is computational intensive and interpolation version is usually used [8].

On the other hand, multi-scale analysis decomposes a signal into different spatial-frequency components. By properly selecting the decomposition filters, desired features of an object can be separated from noise. Therefore we can selectively enhance features of interest by modifying corresponding components in the transform domain.

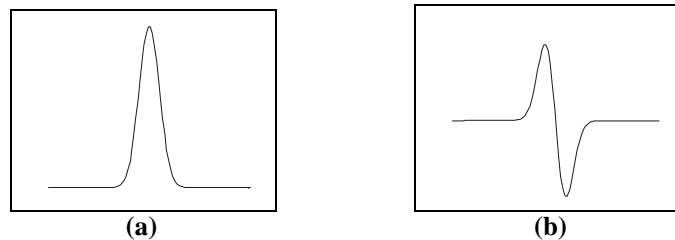


Figure 3: (a) Cubic spline smoothing function $\theta(x)$. (b) Quadratic spline wavelet $\psi(x)$ of compact support defined as the derivative of the smoothing function.

For this work, we used the quadratic spline wavelet function $\psi(x)$, which has compact support and is continuously differentiable. It is the derivative of a cubic spline function $\theta(x)$ (Figure 3). It can be shown that by using a wavelet that is the derivative of a smoothing function the wavelet transform $W_{2^j}^d f$ of the signal f is proportional to the derivative of the signal smoothed at scale 2^j . The wavelet transform can then be considered as an adaptive (scale dependent) detection procedure that finds signal variation points in two orthogonal directions x and y [16]. In addition, the wavelet function we are using, as shown in Figure 3(b), well approximates the first derivatives of a Gaussian function.

In this paper, we introduce contrast enhancement by AHE in a multi-scale paradigm. Depending on the frequency properties of the sub-band images created as a result of an expansion, we apply AHE with different sizes of local windows. There were several factors we took into account in choosing the suitable size of local windows for AHE processing within the sub-band images.

- (1) *The frequency properties of the sub-band.* The coarser levels include more general shape information and should not be changed much. Therefore we apply a relatively large size local window. On the other hand, the finer levels include more local detail information. Therefore relatively smaller local windows are used. In our application, the dyadic wavelet decomposition was used, therefore we chose the local window size to match the dyadic series, which was adapted to the support of the decomposition filters.
- (2) *The size of the image.* Discrete histogram equalization is only an approximation of the analytical case, therefore if the number of pixels for computing the histogram is small, the result will not be stable and will have a large deviation from the theoretical expectation. Also, the size of image also determines the maximum levels in a dyadic wavelet decomposition. In our research, we used high-resolution CT images of 512×512 pixels, and a five-level dyadic decomposition. Thus, the AHE window sizes ranged between 128×128 and 16×16 .

2.2 Evaluation of the MAHE [19]

We first presented readers with enhanced images processed by unsharp masking, HE, AHE, CLAHE (Figure 4), and asked for a qualitatively evaluation. The readers uniformly selected the CLAHE-enhanced images as having enough enhancement without having an uncomfortable amount of artifacts and noise. Therefore we choose CLAHE as our target for comparison.

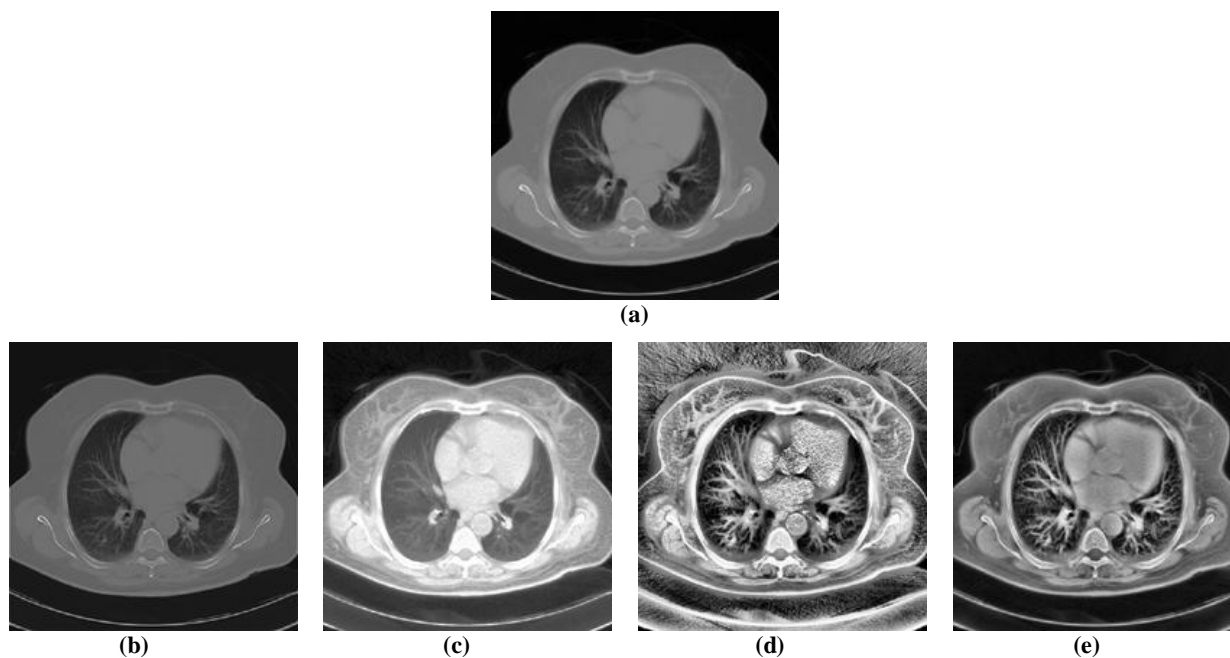


Figure 4: Contrast enhancement by traditional methods. (a) original chest CT image, and enhanced images by (b) unsharp masking, (c) HE, (d) AHE, (e) CLAHE, respectively.

A database of 109 single CT images of the chest was randomly harvested from 40 routine clinical examinations on patients who had various common clinical conditions. Image abnormalities included air cysts (AC), pulmonary nodules (PN), linear densities (LD), ground glass opacities (GGO), lung consolidation (LC), mediastinal lymph nodes (MLN), pericardial effusions (PE), pleural effusions (PLE) and bone lesions (BL).

Each raw file was subsequently processed by MAHE and CLAHE for comparison purposes. A clinical digital reading system in the Department of Radiology, New York Presbyterian Hospital, was used for display.

Three board-certified radiologists, one general and two specialized chest radiologists participated in the evaluation. Each reader was shown the three sets of images, including the original images under conventional window settings for mediastinal, lung and bone tissues respectively. The three sets of images were shown to each reader during three sessions, separated by at least two-week time intervals to avoid recall bias (Dr. W. Huda, personal communication, September 2000). The images at each session were shown in random order to avoid biases of order effects.

As histological correlation was not provided in this study, the ground truth was determined by a consensus of two of the three radiologists' interpretation of each image viewed with conventional window settings.

Performance with conventional windows was compared with the diagnostic performance derived following contrast enhancement with two test conditions, CLAHE and MAHE. Image interpretation times as well as lesion detection rates were compared for conventional windows and the two test enhancement algorithms, and the interpretation time was also recorded for each image.

For comparison of the time required to interpret images using conventional windows, CLAHE and MAHE enhancement, a one-way statistical analysis of variance test was employed. Statistical significance of the consensus readings for each enhanced image compared to conventional windows was determined by a chi-square test. Diagnosis sensitivity and specificity was calculated for all types of lesions as listed. All claims of statistical significance are made at confidence levels $p < 0.05$.

3. RESULTS AND DISCUSSIONS

In Figure 5, we show enhanced images by MAHE and CLAHE with distinct abnormalities. Notice that in (b) and (e), the nodule has been enlarged by the CLAHE, while the MAHE enhanced the nodule appearance, but did not change its size significantly. The appearance of the bronchi structures was enhanced nicely in both CLAHE and MAHE. Again, in the CLAHE-enhanced images, the bronchi shows enlargement and distortion. The radiologists also found that MAHE-enhanced CT images of the chest showed fine interstitial markings in the periphery of the lung, where conventional windows showed no vasculature. We suggest that the interstitial markings are true findings brought out with the algorithm rather than noise. As contrast improvement is gained in each image without sacrificing detail. However, at this time, we have no histological evidence to support this hypothesis.

Table I shows a comparison of the average interpretation time (in seconds) required for each CT image displayed with the three display modes. Interpretation time of MAHE and CLAHE enhanced images are all statistically significant shorter than the conventional window. As we expected, a fully automatic displaying scheme that can display detail information of all type of tissues reduced the reading/interpreting time in clinical diagnosis.

Table I: Comparison of average interpretation times in seconds between the three display modes.

	Conventional Window Settings	CLAHE	MAHE
Reader 1	8.9	7.2	7.2
Reader 2	16.5	12.1	11.1
Reader 3	11.3	9.7	8.1
Average	12.2	9.6	8.8

Since the interpreting results from conventional window display was considered as ground truth, we only compare the diagnosis sensitivity and specificity of the two enhancement results [20]. Unfortunately, because of the limited number of cases from each abnormality, most of them did not reach statistical significance. The only exception is: MAHE was superior to CLAHE for the detection of air cysts (AC). We also observed significance in that CLAHE was superior to MAHE for the detection of small nodules (PN with size less than 1cm), from the discussion with the radiologists, we discovered that after CLAHE enhancement, the size of the nodules appears to be enlarged (Figure 5e). After careful comparison with the conventional windows display, the readers consistently agreed that MAHE enhanced images do not change the size of small nodules (Figure 6). A recognized limitation of CLAHE is that small regions of sharp contrast change in an image are de-emphasized [1, 8]. As a result, in the lung, all structures (pulmonary vessels and nodular opacities) with density against the background of air in the alveoli are enlarged and slightly distorted.

4. CONCLUSIONS AND FUTURE WORK

A multi-scale adaptive histogram equalization method was reported here, which showed promising results on chest CT interpretation. We claimed that the advantage of this method comes from combining the local enhancement ability of AHE, and the selectivity of spatial-frequency components from wavelet analysis. The overall diagnostic sensitivity compares favorable with state-of-art enhancement methods, and also circumvents and reduces some of the artifacts visualized with existing methods. The ability of simultaneously displaying the full dynamic contrast range was shown to be efficient in terms of interpretation time. The diagnostic performance showed the possibility of building a new “Power Windows” scheme for clinical usage.

Following the conventional three-windows settings, we might also tailor the parameters to find the best enhancement for particular abnormalities based on their spatial-frequency properties. Although we would not have the advantage of saving interpretation time, we certainly expect a more reliable diagnosis compared to existing windowing schemes.

Image enhancement with a dyadic wavelet framework has been used successfully [11, 21-23] and tested systematically [24, 25]. Our research extended the previous work by applying new enhancement protocols in consideration of local information.

5. ACKNOWLEDGEMENTS

This work was supported in part by the Whitaker Foundation.

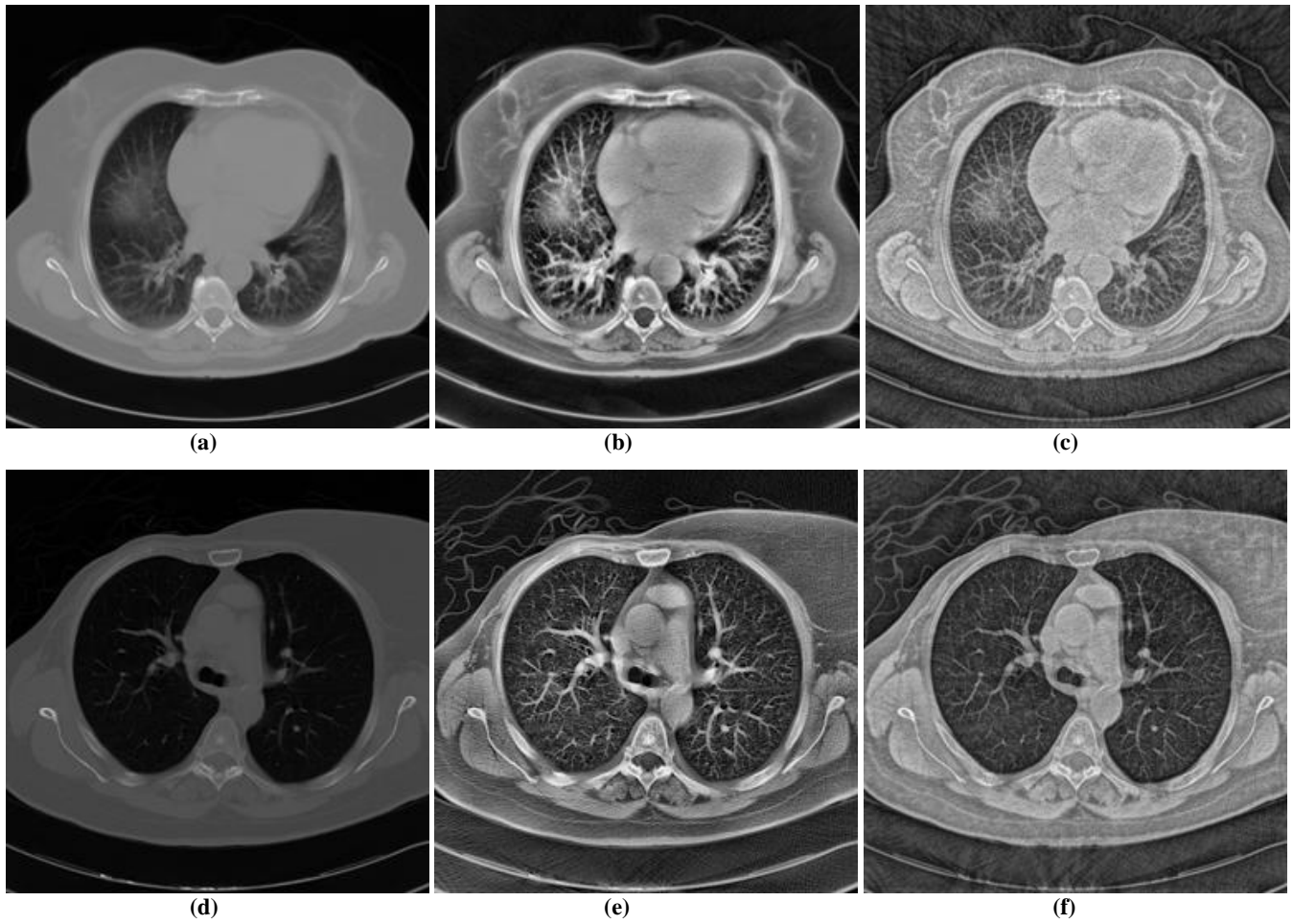


Figure 5: Results of the two enhancement methods. Left column: original image. Center column: CLAHE-enhanced images. Right column: MAHE-enhanced images. (a) bone lesion. (d) bone lesion and nodules.

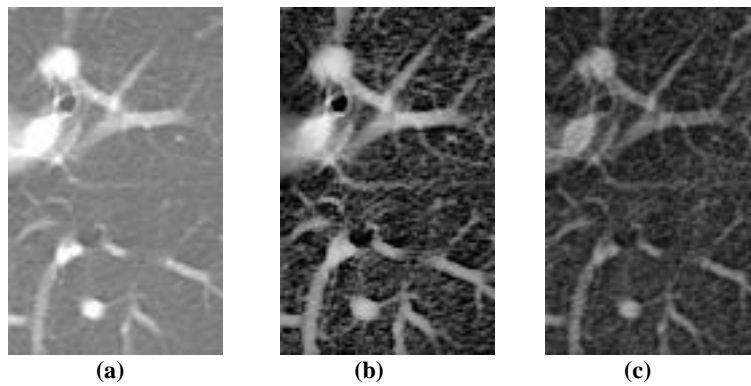


Figure 6: An enlarged display of a chest CT lung region containing detail lung structures and lung nodules. (a) original image displayed in conventional lung window. (b) CLAHE enhanced image. (c) MAHE enhanced image.

6. REFERENCES

- [1] J. B. Zimmerman, S. B. Cousins, K. M. Hartzell, M. E. Frisse, and M. G. Kahn, "A Psychophysical Comparison of Two Methods for Adaptive Histogram Equalization.," *Journal of Digital Imaging*, vol. 2, pp. 82-91, 1989.
- [2] J. E. Barnes, "Characteristics and control of contrast in CT.," *Radiographics*, vol. 12, pp. 825-837, 1992.
- [3] A. K. Jain, *Fundamentals of Digital Image Processing*. Englewood Cliffs, NJ: Prentice-Hall, 1989.
- [4] E. D. Pisano, E. B. Cole, and B. M. H. e. al., "Image Processing Algorithms for Digital Mammography: A Pictorial Essay.," *Radiographics*, vol. 20, pp. 1479-1491, 2000.
- [5] L. Lehr and P. Capek, "Histogram equalization of CT images.," *Radiology*, vol. 154, pp. 163-169, 1985.
- [6] V. Diagalakis, D. G. Manolakis, V. K. Ingle, and A. K. Kok, "Automatic adaptive contrast enhancement for radiological imaging," presented at IEEE International Symposium on Circuits and Systems, 1993.
- [7] S. M. Pizer, J.B.Zimmerman, and E. Staab., "Adaptive grey level assignment in CT scan display.," *Journal of Computer Assistant Tomography*, vol. 8, pp. 300-305, 1984.
- [8] S. M. Pizer and E. P. Amburn, "Adaptive histogram equalization and its variations.," *Computer Vision, Grpahics, and Image Processing*, vol. 39, pp. 355-368, 1987.
- [9] K. Rehm and W. J. Dallas, "Artifact Suppression in Digital Chest Radiographs Enhanced with Adaptive Histogram Equalization," presented at SPIE: Medical Imaging III, 1989.
- [10] M. Unser and A. Aldroubi, "A review of wavelets in biomedical applications," *Proceedings of the IEEE*, vol. 84, pp. 626-638, 1996.
- [11] A. F. Laine, S. Schuler, J. Fan, and W. Huda, "Mammographic feature enhancement by multiscale analysis," *IEEE Transactions on Medical Imaging*, vol. 13, pp. 725-740, 1994.
- [12] A. F. Laine, J. Fan, and S. Schuler, "A framework for contrast enhancement by dyadic wavelet analysis," in *Digital Mammography*, A. G. Gale, S. M. Astley, D. R. Dance, and A. Y. Cairns, Eds. Amsterdam, The Netherlands: Elsevier, 1994, pp. 91-100.
- [13] I. Koren and A. Laine, "A discrete dyadic wavelet transform for multidimensional feature analysis," in *Time Frequency and Wavelets in Biomedical Signal Processing, IEEE Press series in biomedical engineering*, M. Akay, Ed. Piscataway, NJ: IEEE Press, 1998, pp. 425-448.
- [14] P. G. Tahoces, J. Correa, M. Souto, and C. G. and, "Enhancement of chest and breast radiographs by automatic spatial filtering," *IEEE Transactions on Medical Imaging*, vol. 10, pp. 330-335, 1991.
- [15] S. Mallat, *A Wavelet Tour of Signal Processing*. San Diego, CA: Academic Press, 1998.
- [16] S. Mallat and S. Zhong, "Characterization of signals from multiscale edges," *IEEE Transactions on Pattern Analysis and Machine Intelligence*, vol. 14, pp. 710-732, 1992.
- [17] W. T. Freeman and E. H. Adelson, "The design and use of steerable filters," *IEEE Transactions on Pattern Analysis and Machine Intelligence*, vol. 13, pp. 891-906, 1991.
- [18] J. Babaud, A. P. Witkin, M. Baudin, and R. O. Duda, "Uniqueness of the Gaussian kernel for scale-space filtering," *IEEE Transactions on Pattern Analysis and Machine Intelligence*, vol. 8, pp. 26-33, 1986.
- [19] L. Fayad, Y. Jin, N. Shetti, and A. Laine, "The Sharper Image: CT image processing for the radiologist.," presented at European Congress of Radiology, Vienna, Austria, 2001.
- [20] L. Fayad, Y. Jin, A. Laine, Y. Berkmen, G. Pearson, B. Freedman, and R. V. Heertum, "Power Windows for CT: A Potential Wavelet of the future?," *Radiology*, to appear, July 2001.
- [21] A. F. Laine, J. Fan, and S. Schuler, "Contrast enhancement by dyadic wavelet analysis," *Proceedings of IEEE EMBS*, vol. 1, pp. 10a-11a, 1994.
- [22] A. Laine, S. Song, and J. Fan, "Adaptive Multiscale Processing for Contrast Enhancement.," presented at Proceedings of SPIE: Conference on Biomedical Imaging and Biomedical Visualization, San Jose, CA, 1993.
- [23] W. Qian, L. Li, and L. P. Clarke, "Adaptive Directional Wavelet-based CAD method for Mass Detection," in *Computer-Aided Diagnosis in Medical Imaging*, K. Doi, H. MacMahon, M. L. Giger, and K. R. Hoffmann, Eds.: Elsevier Science B.V., 1999, pp. 253-257.
- [24] R. Mekle, A. F. Laine, and Y. Jin, "Wavelet Representations for Digital Mammography," Columbia University, New York, Final Report For U.S. Army Medical Research and Material Command, Fort Detrick, Maryland June 15 1999.
- [25] R. Mekle, A. F. Laine, S. Smith, C. Singer, T. Koenigsberg, and M. Brown, "Evaluation of a Multi-Scale Enhancement Protocol for Digital Mammography," presented at SPIE, Wavelet Applications in Signal and Image Processing VIII, San Diego, 2000.